# Predicting Preferences for Adduct Formation in Electrospray Ionization: The Case Study of Succinic Acid

Stepanovic, Stepan; Hopfgartner, Gerard

**How to cite**

STEPANOVIC, Stepan, HOPFGARTNER, Gerard. Predicting Preferences for Adduct Formation in Electrospray Ionization: The Case Study of Succinic Acid. In: Journal of the American Society for Mass Spectrometry, 2023, vol. 34, n° 4, p. 562–569. doi: 10.1021/jasms.2c00297

This publication URL: https://archive-ouverte.unige.ch/unige:171486
Publication DOI: 10.1021/jasms.2c00297

# Predicting preferences for adduct formation in electrospray ionization: the case study of succinic acid

Stepan Stepanovic and Gérard Hopfgartner*

**ABSTRACT:** A simple theoretical approach is developed, that can be used to predict the preference of ion adducts formation (with alkali $Li^+$, $Na^+$, $K^+$ and alkaline earth $Ca^{2+}$, $Mg^{2+}$ metals) in electrospray ionization mass spectrometry (ESI-MS) of succinic acid, associated with several protonation/deprotonation equilibria. The applied strategy consists of using vacuum environment as well as both implicit and explicit solvation of reactive sites and density functional theory (DFT) as method of choice. These distinct levels of theory mimic the smooth transition between condensed environment and free ion in a gas phase. Good correlation between the Gibbs free energies for protonation/adduct formation processes with the peak observation in the obtained mass spectra provides the insight into the physical basis behind adduct preference and selectivity. This signifies the relationship between microscopic interactions, ionization efficiency and types of ions that reach the detector.

## Introduction

Liquid chromatography coupled to mass spectrometry (LC-MS) using electrospray ionization (ESI) is largely applied for qualitative and quantitative analysis of low molecular weight compounds in metabolism, metabolomics and forensic. Although the most common way for ion formation in ESI is protonation in positive and deprotonation in negative mode, multiple other ionization processes are known such as adducts or homo- and heteromultimers formation. Beside the broad pallets of experimental setups and analyte classes, this also has a downside - the obtained spectra are often complicated due to the ionization by adduct formation with metal or small organic ions.[1, 2] The appearance of multiple adducts makes sample identification more problematic in particular considering that they do not fragment well in collision induced dissociation.[3-5] This is why, in metabolomics, the adducts are typically regarded as unwanted contaminants.[4] Fortunately, since many features are mutually related, statistically grouping correlated features reduces the total number of feature groups.[6] The source of metal adducts remains unclear as they can originate from the solvents, the additives, the sample or the analytical system. In quantitative studies they may decrease the sensitivity by dividing analyte signal across the ion series or affect assay linearity and challenge assay transfer.[4] It has been reported the concentration of sodium in mobile phase does not affect the relative ionization efficiency of $[M+H]^+$ nor $[M+Na]^+$ but the topic remains unclear for multimers or real samples[7]. Furthermore, acidic functional groups are highly represented in metabolites and natural products[8] and are shown to facilitate the adduct formation.[9] Simultaneously, many alkaloids (like cocaine) are basic and do not exhibit preference for adduct formation. It would be highly desirable and very beneficial if the adduct presence could have been rationally predicted for analytes with completely different functional groups and molecular structures.

Adduct annotation methods,[4, 5, 9-11] such as the multi-layered approach,[3] are very powerful for the peak assignation and features reduction, but they do not offer deeper insight into the microscopic mechanisms. By far the most studied metal ion adducts contain $Na^+$ and $K^+$ cations.[12, 13] While $Li^+$ and divalent cations have received much less attention. It is important to note that $[M\cdot Na]^+$ $[M\text{-}H\cdot Mg]^+$ can be easily misassigned since their masses are very similar, although the characteristic $Mg^{2+}$ isotopic pattern can be a clear indication. The same applies for the $K^+$-$Ca^{2+}$ pair. Since we have already observed the formation of $Ca^{2+}$ adducts, that were wrongly assigned as $K^+$ adducts in the literature [3], we decided to investigate whether this is a consequence of stronger ionization efficiency of $Na^+/K^+$ over the other ions, or they are just often present in excess and form the only visible signals in the electrospray ionization mass spectrometry (ESI-MS). Since one of the aims of this paper is to correlate experimental observations with the microscopic interactions, it is instructive to consider the mechanisms involved in solvated analyte path to the MS detector reviewed by Cech *et al.*[14]

The signals observed in the ESI mass spectra are controlled by various equilibria, involving analyte, ions, and solvent molecules, occurring on the path from the solution in ESI needle to the mass detector. The initial step is analyte-ion interaction inside the needle, followed by interactions inside charged nanodroplets. These processes occur in a condensed phase. As already described, succeeding steps include solvent evaporation linked with adduct endurance in the vacuum environment. Unfortunately, even the experimental results are not easily reproducible, and a small change in temperature, capillary/cone voltage, pressure, diverse vendor setups and source geometries can lead to different line intensities observed. As one might guess, it is a very non-trivial task to theoretically model these phenomena and reproduce experimental observations and trends.[15-17]

Even from this short description of the overall process it is clear that the complicated ab-initio molecular dynamics set of calculations would need to be undertaken, in order to model the overall system dynamics and describe the bond breaking-bond making process involved in proton transfer and possible fragmentation properly. On the path toward a simple model that can be used to tackle the ionization preference with the ESI ion source, we further need to consider the relevant processes and their influence on the overall spectra. Should more focus be directed toward the condensed phase interaction in the ESI source, adduct endurance in the vacuum environment or, perhaps, the equilibria within the charged nanodroplets traveling to the MS detector? This is not a trivial question, but one could argue that ion source processes are mainly “setting the stage”, since there are many equilibria taking place between the source and MS detector. As for the desolvation phase, although it is extremely important step, (vide infra), its complexity sets it outside of this manuscripts scope.

Experimentally, the adduct binding constants in condensed phase do not obey the trends observed in ESI/MS.[18] In line with that finding, there are some correlations between ionization efficiency and analyte hydrophobicity. Furthermore, the analyte surfactant properties are very important since it is the excess charge rich parent droplet's surface layer that breaks up into descendants’ droplets. Thus, it is not difficult to conceive that surface-active analytes will follow the surplus charge into the offspring droplets, increasing their ionization efficiency.

Finally, although it is reasonable to expect correlation between solution basicity in a positive mode ESI/MS and ionization efficiency,[19-24] it would be wrong to think that proton transfer occurs only in the condensed phase. Gas phase proton shift occurs when solution phase basicity and gas phase proton affinity are not correlated.[25]

From the description given above, neither the condensed phase equilibrium nor the gas phase interactions or vacuum stability can be a priori ignored. To tackle this complicated problem, we have performed both calculations in vacuum, implicit-solvation and partial explicit solvation of the interaction sites. These different levels of theory correspond to smooth transition between free ion in a gas phase and partial condensed environment. The goal of this manuscript was to evaluate to what extent the observed spectra correlate with the thermodynamics of analyte ion interaction.

This work extends some very interesting research[26-28] regarding $Cs^+$ affinities to the various (mono- and poly-) carboxylic acids. But, beside similar subject (metal-cluster stability estimate, with the help of DFT), it centers around completely

different problem – microscopic mechanism for observed preference in adduct formation and relative peak intensities in MS1 ESI spectra. In this framework, the succinic acid is used just as computationally interesting model system, to tackle the question of protonation vs adduct formation for any given analyte. Since succinic acid gives solely the ion adducts and protonated molecule, has a complicated potential energy surface (with many close lying cyclic and acyclic conformers) and the most important signals also involve carboxylic group deprotonation, it was selected as a test system for our model development.

## Methods

All DFT calculations were performed with the Amsterdam Modelling Suite (AMS2021) program package.[29, 30] Initial structures were refined with global minimization techniques available in AMS, namely Basin Hopping[31] and systematic variation of dihedral angles,[32] using XTB semiempirical methodology.[33] The obtained low energy structures were later reoptimized with PBE DFT method,[34, 35] using full electron TZ2P Slater type orbitals basis, Grimme G4[36] dispersion correction and implicit[37-39] (as well as partial explicit) solvation, until the maximum gradient component was less than $5 \cdot 10^{-4}$ a.u (default is $10^{-3}$). The nature of stationary points is confirmed by calculating analytical Hessians.

Since we essentially describe the adduct formation and the proton transfer, in cases when the species we need are not the most stable (for example, we have one protonation form of reactant while the other is in product, one of them being the more stable one) we performed the constrained optimization. Depending on the desired proton localization, the "natural bond length" was used as constraint. For example, if we use the acetate ion for the deprotonation process, it is more favorable for it to take the succinic acids proton. In order to keep the proton on succinic acid (in the reactant) we optimized it with the preferred bond length in the free succinic acid. We have now explicitly included the constraints description wherever used, and we also provide the example input files.

Experimental spectra were acquired on a TripleTOF 6600+ (Sciex, Concord, ON, Canada) in positive ionization modewith an electrospray ionization (ESI) probe, Optimized ion source parameters were as follows: curtain gas (CUR) was set to 25 psi, nebulizing gas (GS1) was set to 30 psi and drying gas (GS2) was set to 20 psi. Needle voltage (ISVF) was set to 4-5 kV and temperature (TEM) was set to 300 ºC. The raw data were processed with PeakView (v2.2, Sciex). Spectra were averaged and were then centroided and exported as text files.

50% MeCN and 50% MeOH were used as solvents. Solution of pure succinic acid (100µg/mL) was used, unless different concentration is clearly noted (some spectra in SI). When salt solutions are added (only infusion was used at 10-50 µl/min), the following ions were used LiCl, NaCl, KCl, $MgCl_2$, $CaCl_2$ (all with c=2mM). When acetate counter ion or formic acid additive were utilized (again, just few examples in the SI) it was clearly noted and rationalized. All the used compounds are p.a. quality, commercially available and were obtained from: Alfa Aesar (succinic acid, 99+%), ACROS (LiCl, , 99%), Sigma Aldrich (NaOAc, 99%; KCl, minimum 99.0%; NaCl, ≥99.5%), Fluka ($CaCl_2 \cdot 2H_2O$, >99%), Merk ($MgCl_2 \cdot 6H_2O$, >99.5%). The following solvents were used: HPLC-grade acetonitrile (ACN) and methanol (MeOH) from VWR (Darmstadt, Germany); and water from Huberlab (Aesch, Switzerland). No buffer was added, and solution was essentially weakly acidic (100µg/mL≈0.00085M succinic acid and, in one case, 2mM $MgCl_2$ are the only non neutral solution constituents). TOF spectrum were acquired over a range of *m/z* 100 to 1000 with an accumulation time of 250 msec, the declustering potential was set 80 V.

## Results and Discussion

As explained, there are many complicated factors that influence the intensity of a specific ion signal in the mass spectrum.

Since our model system is succinic acid (vide infra) we will shortly describe/illustrate simplified view of some important equilibria for the carboxylic acid containing systems that lead to a $[M+X]^+$ ion observed at the detector (X is metal cation or $H^+$). We have chosen general carboxylic acid to demonstrate the most important points, since that enables us to ignore conformational flexibility and possible chelate complexes. The equilibria that involves protonation/adduct formation and subsequent 'naked ion' formation (whose signal is observed at the detector) is conceptually sketched on Figure 1. On Figure 1-a, we have depicted the protonation process, on Figure 1-b the adduct formation with the one-valent metal cations, and, finally,

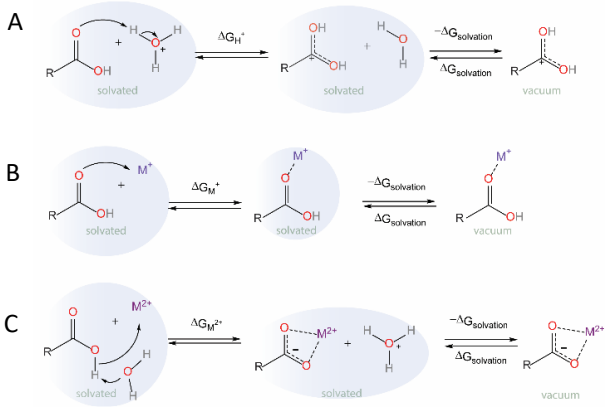


the adduct formation with two-valent cation, coupled with deprotonation process, can be seen on Figure 1-C.

*Figure 1: Schematic representation of protonation and adduct formation with metal ions, for general carboxylic acid as the simplest model system. $M^+/M^{2+}$ represents singly or doubly charged metal cation and the curved (double-headed) shows the movement of an electron pair. Dashed line between the metal and anionic oxygens represents an ionic interaction, while the dashed double bond in second and third structure (parts a) and b)) demonstrates a resonance stabilization of carboxylic ions.*

Protonation, metal binding and (possible) deprotonation processes are represented as condensed phase equilibria, and described by appropriate ΔG value (left portion of Figure 1-a, b and c). The second step in the equations show in the Figure 1 IS depicted as just desolvation of adduct formed in the previous step. Cleavage of carboxylic acid-metal ion adducts in a vacuum state seems unlikely because their association energies are very negative thus, this process is not included in the sketch. It

is important to note that the desolvation phase is not a simple equilibration process, but a dynamic declustering behavior, governed by kinetic energy (dependent on the excess charge and electric field, among other factors) and vacuum environment. It probably involves, beside solvent evaporation, Coulomb fissions and/or field desorption of some solvated ions. This is the most complicated step in the ion path that is responsible for many patterns observed in the spectra and cannot be easily modeled. This phase must be modeled with molecular dynamics (MD), and, preferably, using at least some semi-empirical Hamiltonian (if not DFT/ab-initio) to tackle proton transfer, ion binding and any possible ion breaking with the appropriate quantum mechanical description.

In this work, we have modeled the thermodynamics of condensed phase proton transfer and adduct formation processes, to check for possible correlation with ionization efficiency and some patterns observed in the spectra. The proposed approach, which is explained in detail later on, is very straightforward – consisting on microsolvation of reaction centers, treated with DFT optimization with implicit, COnductor-like Screening MOdel (COSMO) solvation included. It is also easily extendable and applicable to other small to medium sized systems. The possible complication arises with conformationally very flexible molecules, and potential multidentate analytes since there is a need to properly explore the very complicated Potential Energy (hyper)Surfaces (PES). With the surge of automatized methods nowadays, majority of the process can be automated, including for example, screening of multiple protonation/deprotonation/ion binding sites.

Beside already described properties, the succinic acid was selected as the main model because it represents a very challenging system for computational modelling. It has considerable flexibility and even the opportunity to coordinate the proton/metal ion with two sides and two oxygens on each carboxylic group. Thus, there are a plethora of combinations to form complicated local minima on PES. The general pathways regarding proton transfer/adduct formation are similar as the ones shown on the Figure 1 for the general carboxylic acid. What differs is the possibility for many close-lying conformers and chelation and bridging ligation.

Standard ESI-MS spectra of succinic acid can be seen on Figure 2- a). Most of the peaks originate from the adduct ions of the form $[(succ)_p(succ\text{-}H)_{(m\cdot n-1)}(M^{n+})_m]^+$, i.e. succinic acid can be in neutral or deprotonated form, depending on the metal charge and count, so the total charge of the complex is **+1**. Protonated succinic acid is not observed.

As in many situations, adduct ions are normally present (predominant!) in the spectra, and they usually originate from the glassware (current case) but can also come from solvent impurities and coupled HPLC. This indicates that there is a large predominance toward ion adduct formation compared to the protonation process. This seems very natural if we look at the basic chemical properties: succinic acid is very weakly basic but has a lot of oxygen atoms with high affinity toward metal coordination (which even increases after facile deprotonation). On the other hand, there is an abundance of examples showing that basic molecules have (often predominant) signal of protonated analyte. This directed us to examine how important is a simple quantity such as ΔG(proton/ion – adduct) interaction in the extremely complicated ESI-MS setup. This limited the scope of the investigation significantly, since it is clear that many effects that influence signal presence and intensity are concentration dependent. Simple example can be seen on on Figure 2, which, again, depicts the ESI-MS spectra of succinic acid, but this time with added 2mM LiCl, NaCl, KCl, $MgCl_2$ and $CaCl_2$. It is clear that, as expected, only the adducts with the cations from the supplemented salt became visible, and the various small concentration salts from glassware impurities are no longer detectable. We will focus little bit on spectra with added NaCl(Figure 2- c))we can see that many sodium adduct peaks can be observed. Interested readers are directed toward literature,[12] but also the paragraph on page S2 in Supporting Information (SI), where one can also find more data and better insight on Figures S1and S2 (the change of succinic acid ESI-MS spectra with constant NaCl concentration and varying the amount of succinic acid is displayed). Figure S3 demonstrates what happens when the acid concentration is kept constant and the amount of NaCl is varied. In order to (at least to some extent) reduce the concentration influence on ion competition for adduct formation, we used 2mM concentration for all salts.

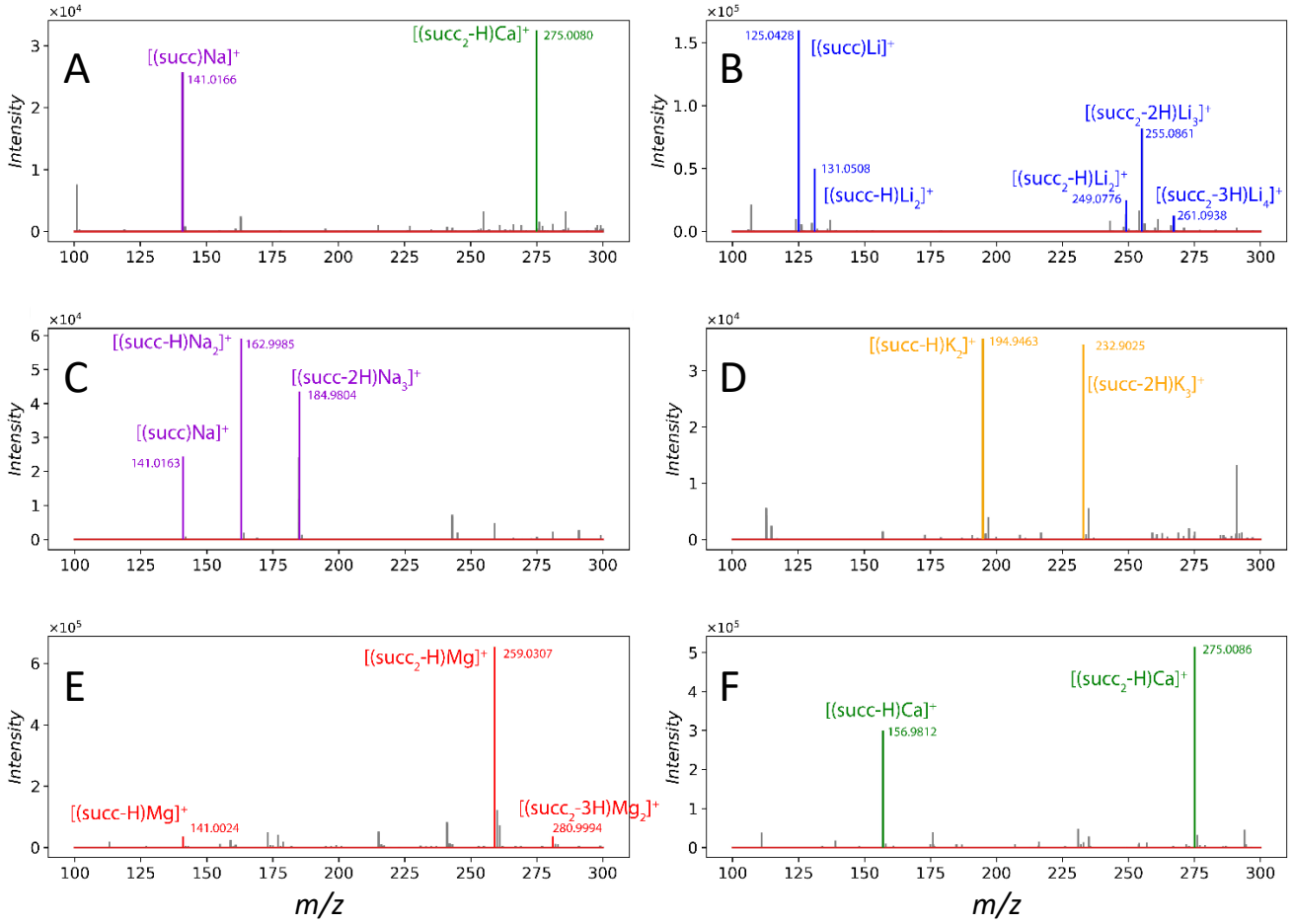


*Figure 2: Mass spectra of succinic acid dissolved in 50% methanol, a). b) shows succinic acid + LiCl, c) is succinic acid+ NaCl, d) displays th spctra of succinic acid +KCl. Finally, on e) we can see succinic acid+ $MgCl_2$ and f) depicts succinic acid +$CaCl_2$*

The described acid-salt relative concentration effects are strictly dynamical phenomena and cannot be treated with "static" quantum mechanical (QM) methods. Since the aim was to propose a simple, smoothly applicable and easily extendable approach, we restricted our model to appropriate reactive site micro solvation (in order to obtain comparable energies for both protonation, deprotonation and ion binding processes), structure relaxation and ΔG estimation using DFT. The experimental spectra in SI (Figures S1-S3) clearly demonstrate that the preference of larger vs smaller multimers, and their composition are strictly concentration-dependent phenomena! Thus, it is pointless to address that question with a static approach and cluster stability arguments. But, it is possible to compare the stability of various metal acid adducts, take the deprotonation into account (which is necessity in order to form an adduct with multiply charged cations), correlate that with the protonation process and associate all these facts with the observed ions in the ESI-MS spectra. This approach has the potential to provide a scientifically reasonable estimate not only whether ion adduct formation will be preferable compared to the protonation process, but also the different affinity of single and multiple charged cations.

As it is mentioned in the introduction, the examined cations were selected in order to test their preference of adduct formation, and analyze the results correlation with almost exclusive reports of $Na^+/K^+$ adducts and lack of representation of other ions. Thus, in this investigation we have analyzed the preference of succinic acid for a series of mono-valent ($Li^+$, $Na^+$ and $K^+$) and di-valent ($Mg^{2+}$ and $Ca^{2+}$) metal ions. We have complemented the experimental results with the set of DFT calculations that provides the microscopic insight and cluster stability arguments. The spectra were recorded in two different solvent mixtures MeOH/$H_2O$ (50%) and MeCN/$H_2O$ (50%), and, all ions are added in 2mM concentration as chloride salts (acetate counter ions facilitate formation of pronounces conglomerate structures and complicate the spectra, see SI Figure S4 and S5 and appropriate paragraph).

The detailed and fully annotated list of all the succinic acid-salt mixtures are given in the Supplemental Info, Figures S6-S11, in both solvent mixtures, together with the description of the observed patterns. In short, similar types of adducts can be found as in on Figure 2, i.e. $[(succ)_p(succ\text{-}H)_{(m\cdot n-1)}(M^{n+})_m]^+$. Only the adducts formed by the added salt are observed, since the ions from impurities and glassware are suppressed because of their low concentration. In order to compare the affinity for particular ions, the spectra of ion mixture (all with equal conc. of 2mM) have also been recorded, and can be seen on Figure 3 and Figure S11.

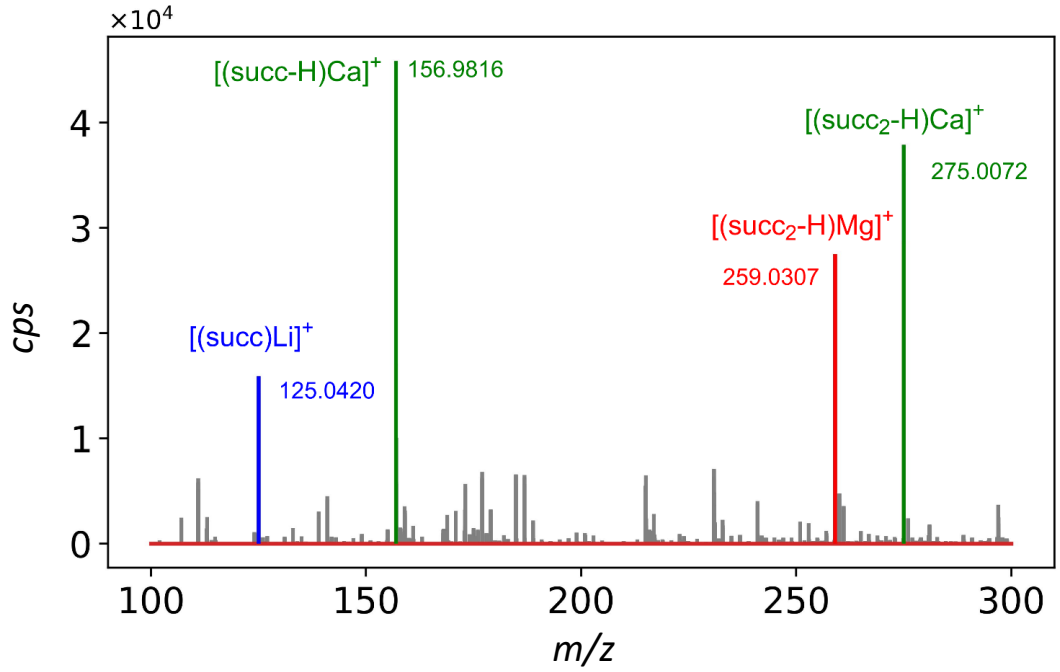


*Figure 3: Mixture of LiCl, NaCl, KCl, $MgCl_2$, $CaCl_2$ (c=2mM) and succinic acid (100µg/mL) in MeOH/$H_2O$ (50%)*

It can be seen that the peaks that dominate the spectra (most intensive ones) are from $M^{2+}$ ion adducts and that only somewhat intense $M^+$ adduct is with $Li^+$ ion. Protonated succinic acid is not observed. It is obvious that the adducts charge density plays an important role. Thus, it can be expected to obtain reasonable results with the theoretical approach that captures the interaction energy, which is an important contribution to ionization efficiency.

To construct a simple but appropriate model system, it was important to note that (most favorable) protonation site and deprotonation center are adjacent carboxylic oxygens. Therefore, we need to be able to accurately model and compare two different proton transfer events as well as the ion coordination. In order to achieve that, we have treated all important interaction centers with two explicit water molecules. The model is depicted on Figure 4.

On Figure 4-a we can see a $Ca^{2+}$ and $Mg^{2+}$ ions binding model, coupled with the deprotonation process (it is clearly depicted which bonds swap from covalent to the H-bond and the other way around). Figure 4-b demonstrates the $M^+$ ion binding, where $H^+$ is also included. It should be noted that neither actual coordinated nor solvated proton are in tetrahedral environment, since it is very unfavorable. More detail about the calculations involved, together with coordinates of all optimized structures can be found in the SI, pages S15-S26.

Although it was mentioned that oligomeric adducts will not be analyzed, since their prevalence is highly concentration dependent, the adduct with two $M^+$ cations and deprotonated succinic acid is also included. It was done for one important reason: to be able to fairly compare $M^+$ and $M^{2+}$ ions, since ΔG for $M^{2+}$also includes the deprotonation process (and taking accurate energetic contribution of deprotonation is not a trivial task). The adducts formed with two $M^+$ cations and deprotonated succinic acid are depicted on Figure 4-c.

The effort was invested to access only relevant processes. For example, a care was undertaken to avoid additional H-bond formation between the water molecules solvating different interaction centers, for more details see SI, pages S-15-S26. Gibbs free energies for the metal/proton binding reactions schematically depicted on Figure 4 are given in Table 1. Electronic energies, that follow identical trends, are given in the SI, Table S1.

*Table 1 Gibbs free energies for the processes depicted in Figure 4. All energies are given in kcal/mol*

| | ΔG PBE | ΔG B3LYP |
|---|---|---|
| $[(succ\text{-}H)\cdot Ca]^+$ | -18.1 | -17.0 |
| $(succ\text{-}H)\cdot Mg]^+$ | -30.9 | -32.1 |
| $[(succ\text{-}H)\cdot 2K]^+$ | 10.8 | 12.0 |
| $[(succ\text{-}H)\cdot 2Li]^+$ | -16.5 | -16.4 |
| $[(succ\text{-}H)\cdot Na]^+$ | -2.8 | -3.2 |
| $[succ\cdot H]^+$ | -0.3 | 1.9 |
| $[succ\cdot K]^+$ | 6.3 | 6.4 |
| $[succ\cdot Li]^+$ | -7.9 | -8.4 |
| $[succ\cdot Na]^+$ | 0.2 | 0.4 |

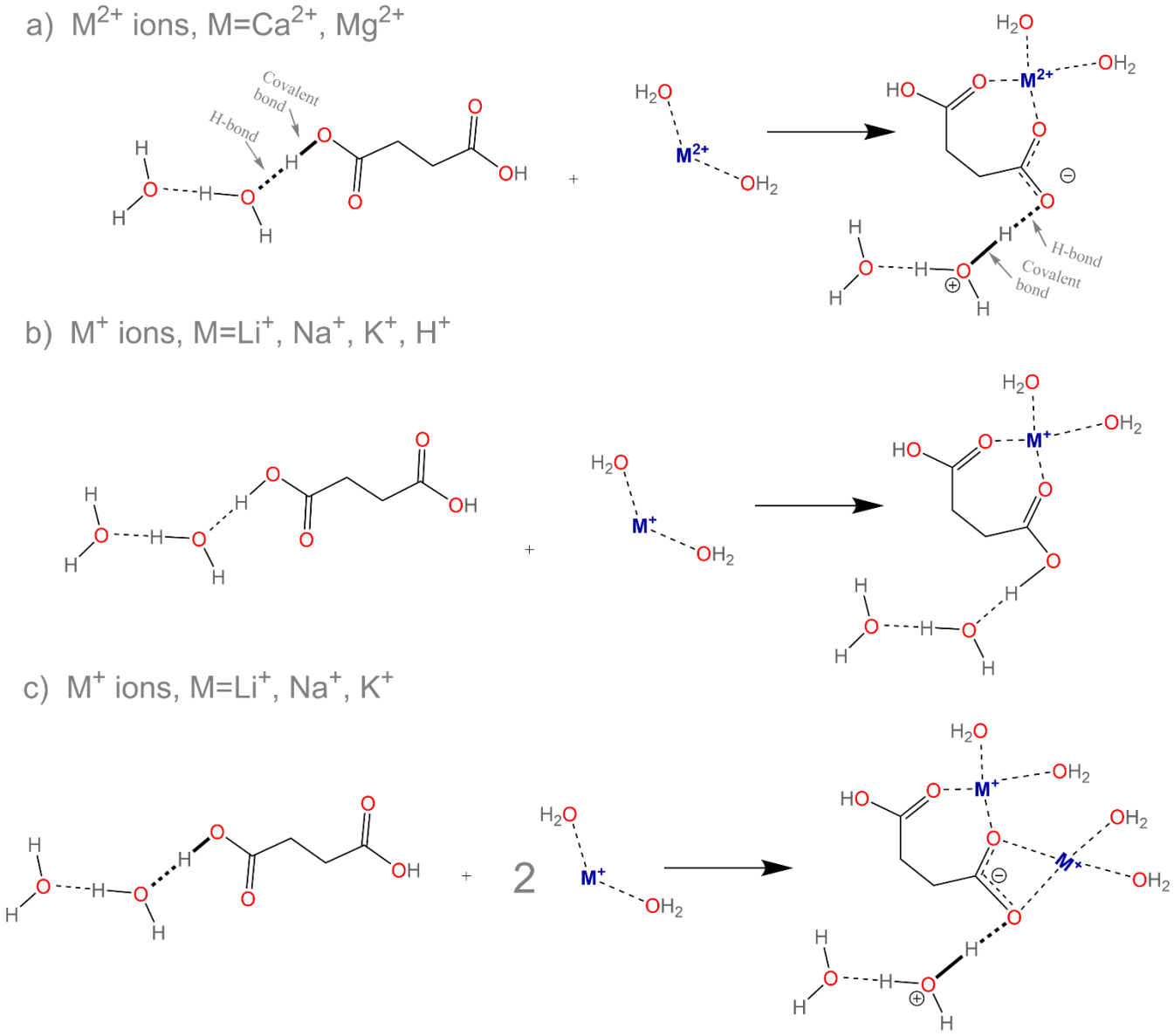


*Figure 4: Model system for succinic acid ion binding*

Simple inspection demonstrates that $M^{2+}$ ions bind more favorably to succinic acid than $M^{+}$ ions and that acid protonation is among the least favorable options. Within the $M^{+}$ ions, $Li^{+}$ gives by far the most stable adduct. These results perfectly corroborate the general trends observed in experimental ESI-MS spectra, Figure 3.

In order to test applicability of the developed approach, it has also been utilized on 1,3,7-trimethyluric acid, which can show the presence of metal adducts, but, the protonated molecule is the dominant line in the spectra. The results can be found in the SI (Figure S13 and Table S3, on pages S15 and S16), and they further demonstrate that simple thermodynamics of protonation/adduct formation correlates well with ionization efficiency, and has the possibility to explain qualitative trends from ESI-MS spectra.

Furthermore, it is necessary to once again state discrepancies between some trends in cluster/adduct stabilities and experimental spectra. First of all, although it is captured that $M^{2+}$ ions dominate the MS spectra, it is crucial to note that $Ca^{2+}$ peaks are more pronounced than the ones from $Mg^{2+}$, which doesn't follow the trend in Gibbs free energy. Furthermore, although almost all the ion adducts are more favorable than the protonation process, the $K^{+}$ ion is an exception. This is no surprise since it would be naive to expect that small and constant micro solvation can fully accommodate $H^{+}$, $Li^{+}$, and $K^{+}$ which is completely different in terms of size and charge density. All these, and many other observations, just confirm that molecule-proton/ion affinity is an important factor in a much broader and more complicated process that determines the overall look of ESI-MS spectra.

In the last few paragraphs, we correlated the results from the salt mixtures (Figure 3) with the thermodynamics of

protonation/adduct formation (Table 1). Can the similar trend be extracted from the single salt solutions? It may be instructive to note the most intensive peaks in the salt solutions, Figure 2/Figures S5-S11. The most intensive peaks are with $Mg^{2+}$ and $Ca^{2+}$ (respectively), then $Li^+$ followed by $Na^+$ and $K^+$. Thus, peak intensities of distinct succinic acid+salt solutions nicely follow the trends from Table 1. Indicated result corroborate the assumption that our model captures important contributions to ionization efficiency. This paves the way toward rational prognosis of small molecule tendency toward protonation / adduct formation, as well as relative adduct signal intensities.

Finally, it is necessary to address simple vacuum and COSMO calculations, as well as the choice of base for the deprotonation step, in order to rationally evaluate the importance in the influence of explicit solvation treatment and model extendibility when different salts are used. The obtained values can be seen in Table 2. Despite the fact that the trends between ions are still similar (since they are caused by metals charge densities), the vacuum results demonstrate unnatural stabilization of $M^{2+}$ adducts which is a consequence of vacuum $M^{2+}$ instability. Both COSMO and vacuum results show weaker agreement with experimental spectra for $Li^+$ ion and the protonation. Better perspective and a qualitative intuition of the relative contribution importance (COSMO, vacuum, explicit solvation, electronic and Gibbs free energy, different functionals) is provided in SI, Table S3 and the accompanying text.

*Table 2: Electronic energies for the vacuum and COSMO calculations , for the processes depicted in Figure S12 and Figure 4. All energies are given in kcal/mol*

| | Vacuum ΔE, PBE | COSMO ΔE, PBE |
|---|---|---|
| $[(succ\text{-}H)\cdot Ca]^+$ | -176.5 | -27.9 |
| $(succ\text{-}H)\cdot Mg]^+$ | -288.8 | -56.0 |
| $[(succ\text{-}H)\cdot 2K]^+$ | 19.7 | 12.9 |
| $[(succ\text{-}H)\cdot 2Li]^+$ | -38.9 | -22.5 |
| $[(succ\text{-}H)\cdot Na]^+$ | -3.1 | 2.1 |
| $[succ\cdot H]^+$ | -44.7 | -12.6 |
| $[succ\cdot K]^+$ | -32.2 | -11.1 |
| $[succ\cdot Li]^+$ | -63.5 | -32.4 |
| $[succ\cdot Na]^+$ | -43.7 | -16.9 |

Regarding the choice of base for the deprotonation step, it needs to be stressed out that we only used water for simplicity and universality but we by no means claim that the actual deprotonation mechanism involves only water molecules. We whish to emphasize that in case that basic anions are present, it is much more reasonable for them to be used.[40, 41] We provide electronic energies and some additional comments, for the adduct formation processes described in Figure 4, with water molecules, chloride anion and acetate anion as bases involved in deprotonation process in the Supplemental Info (as Figure S 14-15 and Table S 4).

Conclusion

The approach for estimation of analyte preference for metal adduct formation vs protonation is given. The model is applied on succinic acid but it is simple and easily extendable procedure. It consists of ΔG estimation for the processes of interest using explicitly solvated interaction center and DFT as chosen methodology. The outlined results reasonably follow many experimental trends and preferences, demonstrating that tendency for adduct formation is an important contribution to ionization efficiency. Furthermore, it experimentally demonstrated and theoretically confirmed that $M^{2+}$ ion adducts should no longer be neglected, especially when analytes possess strongly coordinating functional groups. Thus, looking across the periodic table and focusing into the cationic pairs, like $Na^+/(Mg\text{-}H)^+$ and $K^+/(Ca\text{-}H)^+$, low resolution spectra makes is difficult to distinguish between them, even with the different isotopic pattern. This approach provides a simple microscopic insight into the nature of adduct formation and give us the presumption which one should we expect in the final spectra.

## ASSOCIATED CONTENT

### Supporting Information

Additional experimental spectra, Tables and comments, XYZ coordinates and electronic energies of all calculated structures

## AUTHOR INFORMATION


### Corresponding Author

**Gérard Hopfgartner** − *Life Sciences Mass Spectrometry, Department of Inorganic and Analytical Chemistry, University of Geneva, CH-1211 Geneva 4, Switzerland.*

*orcid.org/0000-0002-9087-606X*

*email: gerard.hopfgartner@unige.ch*

### Author

**Stepan Stepanovic** − *Life Sciences Mass Spectrometry, Department of Inorganic and Analytical Chemistry, University of Geneva, CH-1211 Geneva 4, Switzerland. Institute of Chemistry, Technology and Metallurgy, University of Belgrade, Njegoševa 12, 11000 Belgrade, Serbia*


### Author Contributions

The manuscript was written through contributions of all authors. All authors have given approval to the final version of the manuscript

## ACKNOWLEDGMENT


The authors would like to thank to Ali Ben Hammou for the help in obtaining the experimental spectra of 1,3,7-trimethyluric acid (Figure S13), and Olivera Stepanovic for the comments on the manuscript. The present project was funded by the Swiss National Science Foundation grant 200021_192306.

Insert Table of Contents artwork here

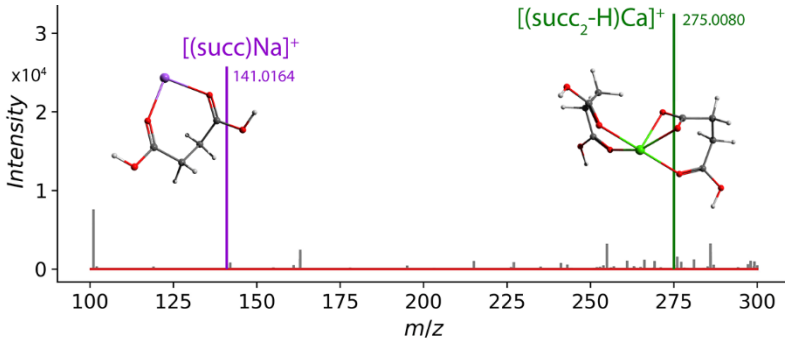


## REFERENCES


1. Carnevale Neto, F., V. Pascua, and D. Raftery, *Formation of sodium cluster ions complicates liquid chromatography–mass spectrometry metabolomics analyses.* Rapid Communications in Mass Spectrometry, 2021. **35**(20): p. e9175.
2. Erngren, I., et al., *Improved Sensitivity in Hydrophilic Interaction Liquid Chromatography-Electrospray-Mass Spectrometry after Removal of Sodium and Potassium Ions from Biological Samples.* Metabolites, 2021. **11**(3): p. 170.
3. Bonner, R. and G. Hopfgartner, *Annotation of complex mass spectra by multi-layered analysis.* Analytica Chimica Acta, 2022. **1193**: p. 339317.
4. Stricker, T., et al., *Adduct annotation in liquid chromatography/high-resolution mass spectrometry to enhance compound identification.* Anal Bioanal Chem, 2021. **413**(2): p. 503-517.
5. Lu, W., et al., *Improved Annotation of Untargeted Metabolomics Data through Buffer Modifications That Shift Adduct Mass and Intensity.* Analytical Chemistry, 2020. **92**(17): p. 11573-11581.
6. Mahieu, N.G. and G.J. Patti, *Systems-Level Annotation of a Metabolomics Data Set Reduces 25 000 Features to Fewer than 1000 Unique Metabolites.* Analytical Chemistry, 2017. **89**(19): p. 10397-10406.
7. El Abiead, Y., et al., *Heterogeneous multimeric metabolite ion species observed in LC-MS based metabolomics data sets.* Analytica Chimica Acta, 2022. **1229**: p. 340352.
8. Skonberg, C., et al., *Metabolic activation of carboxylic acids.* Expert Opinion on Drug Metabolism & Toxicology, 2008. **4**(4): p. 425-438.
9. Broeckling, C.D., et al., *Enabling Efficient and Confident Annotation of LC−MS Metabolomics Data through MS1 Spectrum and Time Prediction.* Analytical Chemistry, 2016. **88**(18): p. 9226-9234.
10. Domingo-Almenara, X., et al., *Annotation: A Computational Solution for Streamlining Metabolomics Analysis.* Analytical Chemistry, 2018. **90**(1): p. 480-489.
11. Misra, B.B., *New software tools, databases, and resources in metabolomics: updates from 2020.* Metabolomics, 2021. **17**(5): p. 49.
12. Erngren, I., et al., *Adduct formation in electrospray ionisation-mass spectrometry with hydrophilic interaction liquid chromatography is strongly affected by the inorganic ion concentration of the samples.* Journal of Chromatography A, 2019. **1600**: p. 174-182.
13. Janda, M., et al., *Determination of Abundant Metabolite Matrix Adducts Illuminates the Dark Metabolome of MALDI-Mass Spectrometry Imaging Datasets.* Analytical Chemistry, 2021. **93**(24): p. 8399-8407.
14. Cech, N.B. and C.G. Enke, *Practical implications of some recent studies in electrospray ionization fundamentals.* Mass Spectrometry Reviews, 2001. **20**(6): p. 362-387.
15. Konermann, L., R.G. McAllister, and H. Metwally, *Molecular Dynamics Simulations of the Electrospray Process: Formation of NaCl Clusters via the Charged Residue Mechanism.* The Journal of Physical Chemistry B, 2014. **118**(41): p. 12025-12033.
16. Konermann, L., et al., *How to run molecular dynamics simulations on electrospray droplets and gas phase proteins: Basic guidelines and selected applications.* Methods, 2018. **144**: p. 104-112.
17. Tabet, J.-C., et al., *Combining Chemical Knowledge and Quantum Calculation for Interpreting Low-Energy Product Ion Spectra of Metabolite Adduct Ions: Sodiated Diterpene Diester Species as a Case Study.* Journal of the American Society for Mass Spectrometry, 2021. **32**(10): p. 2499-2504.
18. Breitbach, Z.S., et al., *Mechanisms of ESI-MS Selectivity and Sensitivity Enhancements When Detecting Anions in the Positive Mode Using Cationic Pairing Agents.* Analytical Chemistry, 2010. **82**(21): p. 9066-9073.

19. Liigand, P., et al., *30 Years of research on ESI/MS response: Trends, contradictions and applications.* Analytica Chimica Acta, 2021. **1152**: p. 238117.
20. Henriksen, T., et al., *The relative influences of acidity and polarity on responsiveness of small organic molecules to analysis with negative ion electrospray ionization mass spectrometry (ESI-MS).* Journal of the American Society for Mass Spectrometry, 2005. **16**(4): p. 446-455.
21. Huffman, B.A., M.L. Poltash, and C.A. Hughey, *Effect of Polar Protic and Polar Aprotic Solvents on Negative-Ion Electrospray Ionization and Chromatographic Separation of Small Acidic Molecules.* Analytical Chemistry, 2012. **84**(22): p. 9942-9950.
22. Cech, N.B., J.R. Krone, and C.G. Enke, *Predicting Electrospray Response from Chromatographic Retention Time.* Analytical Chemistry, 2001. **73**(2): p. 208-213.
23. Ghosh, B. and A.D. Jones, *Dependence of negative-mode electrospray ionization response factors on mobile phase composition and molecular structure for newly-authenticated neutral acylsucrose metabolites.* Analyst, 2015. **140**(19): p. 6522-6531.
24. Golubović, J., et al., *Structure–response relationship in electrospray ionization-mass spectrometry of sartans by artificial neural networks.* Journal of Chromatography A, 2016. **1438**: p. 123-132.
25. Kebarle, P. and M. Peschke, *On the mechanisms by which the charged droplets produced by electrospray lead to gas phase ions.* Analytica Chimica Acta, 2000. **406**(1): p. 11-35.
26. Mayeux, C., et al., *Interaction of the Cesium Cation with Mono-, Di-, and Tricarboxylic Acids in the Gas Phase. A Cs+ Affinity Scale for Cesium Carboxylates Ion Pairs.* Journal of the American Society for Mass Spectrometry, 2009. **20**(10): p. 1912-1924.
27. Maria, P.-C., et al., *Investigations of cluster ions formed between cesium cations and benzoic, salicylic and phthalic acids by electrospray mass spectrometry and density-functional theory calculations. Toward a modeling of the interaction of Cs+ with humic substances.* Rapid Communications in Mass Spectrometry, 2005. **19**(4): p. 568-573.
28. Maria, P.-C., et al., *Bonding energetics in clusters formed by cesium salts: a study by collision-induced dissociation and density functional theory.* Rapid Communications in Mass Spectrometry, 2006. **20**(13): p. 2057-2062.
29. E.J. Baerends, T.Z., A.J. Atkins, J. Autschbach, O. Baseggio, D. Bashford, A. Bérces, F.M. Bickelhaupt, C. Bo, P.M. Boerrigter, C. Cappelli, L. Cavallo, C. Daul, D.P. Chong, D.V. Chulhai, L. Deng, R.M. Dickson, J.M. Dieterich, F. Egidi, D.E. Ellis, M. van Faassen, L. Fan, T.H. Fischer, A. Förster, C. Fonseca Guerra, M. Franchini, A. Ghysels, A. Giammona, S.J.A. van Gisbergen, A. Goez, A.W. Götz, J.A. Groeneveld, O.V. Gritsenko, M. Grüning, S. Gusarov, F.E. Harris, P. van den Hoek, Z. Hu, C.R. Jacob, H. Jacobsen, L. Jensen, L. Joubert, J.W. Kaminski, G. van Kessel, C. König, F. Kootstra, A. Kovalenko, M.V. Krykunov, P. Lafiosca, E. van Lenthe, D.A. McCormack, M. Medves, A. Michalak, M. Mitoraj, S.M. Morton, J. Neugebauer, V.P. Nicu, L. Noodleman, V.P. Osinga, S. Patchkovskii, M. Pavanello, C.A. Peeples, P.H.T. Philipsen, D. Post, C.C. Pye, H. Ramanantoanina, P. Ramos, W. Ravenek, M. Reimann, J.I. Rodríguez, P. Ros, R. Rüger, P.R.T. Schipper, D. Schlüns, H. van Schoot, G. Schreckenbach, J.S. Seldenthuis, M. Seth, J.G. Snijders, M. Solà, M. Stener, M. Swart, D. Swerhone, V. Tognetti, G. te Velde, P. Vernooijs, L. Versluis, L. Visscher, O. Visser, F. Wang, T.A. Wesolowski, E.M. van Wezenbeek, G. Wiesenekker, S.K. Wolff, T.K. Woo, A.L. Yakovlev, *ADF* 2021, SCM, Theoretical Chemistry, Vrije Universiteit, http://www.scm.com: Amsterdam, The Netherlands.
30. te Velde, G., et al., *Chemistry with ADF.* Journal of Computational Chemistry, 2001. **22**(9): p. 931-967.
31. Wales, D.J. and J.P.K. Doye, *Global Optimization by Basin-Hopping and the Lowest Energy Structures of Lennard-Jones Clusters Containing up to 110 Atoms.* The Journal of Physical Chemistry A, 1997. **101**(28): p. 5111-5116.
32. Michał Handzlik, B.v.B., Patrick Melix, Robert Rüger, Tomáš Trnka, Lars Ridder, Felipe Zapata, *PLAMS*. SCM, Theoretical Chemistry, Vrije Universiteit: Amsterdam, The Netherlands.
33. Bannwarth, C., et al., *Extended tight-binding quantum chemistry methods.* WIREs Computational Molecular Science, 2021. **11**(2): p. e1493.
34. Perdew, J.P., K. Burke, and M. Ernzerhof, *Generalized Gradient Approximation Made Simple.* Physical Review Letters, 1996. **77**(18): p. 3865-3868.
35. Perdew, J.P., K. Burke, and M. Ernzerhof, *Generalized Gradient Approximation Made Simple [Phys. Rev. Lett. 77, 3865 (1996)].* Physical Review Letters, 1997. **78**(7): p. 1396-1396.
36. Caldeweyher, E., et al., *A generally applicable atomic-charge dependent London dispersion correction.* The Journal of Chemical Physics, 2019. **150**(15): p. 154122.
37. Klamt, A., *Conductor-like Screening Model for Real Solvents: A New Approach to the Quantitative Calculation of Solvation Phenomena.* The Journal of Physical Chemistry, 1995. **99**(7): p. 2224-2235.
38. Klamt, A. and G. Schüürmann, *COSMO: a new approach to dielectric screening in solvents with explicit expressions for the screening energy and its gradient.* Journal of the Chemical Society, Perkin Transactions 2, 1993(5): p. 799-805.
39. Klamt, A. and V. Jonas, *Treatment of the outlying charge in continuum solvation models.* The Journal of Chemical Physics, 1996. **105**(22): p. 9972-9981.
40. Chu, I.K., T.-C. Lau, and K.W. Michael Siu, *Intraionic, interligand proton transfer in collision-activated macrocyclic complex ions of nickel and copper.* Journal of Mass Spectrometry, 1998. **33**(9): p. 811-818.
41. Rodriquez, C.F., et al., *A possible origin of [M − nH + mX](m−n)+ ions (X = alkali metal ions) in electrospray mass spectrometry of peptides.* International Journal of Mass Spectrometry, 1999. **192**(1): p. 303-317.